Arabian Journal of Chemistry (2018) **11**, 1–13

King Saud University

Arabian Journal of Chemistry

www.ksu.edu.sa
www.sciencedirect.com

ORIGINAL ARTICLE

The electrochemical synthesis and corrosion behaviour of TiO_2/poly(indole-co-aniline) multilayer coating: Experimental and theoretical approach

Serap Toprak Döşlü [a,*], Başak Doğru Mert [b], Birgül Yazıcı [b]

[a] *Mardin Artuklu University, School of Health, Department of Nutrition and Dietetics, Mardin, Turkey*
[b] *Çukurova University, Science and Letters Faculty, Chemistry Department, 01330 Balcalı, Adana, Turkey*

Received 30 September 2016; accepted 15 March 2017
Available online 21 March 2017

KEYWORDS

Stainless steel;
Polymer;
Electrochemical impedance spectroscopy (EIS)

Abstract The aim of this study was to protect stainless steel against corrosion via poly (indole-co-aniline) with the help of titanium dioxide pre-coating. Different monomer ratios (1:1 and 1:9) were applied in order to determine the suitable chain composition to synthesize the copolymer in lithium perchlorate containing acetonitrile. The structures, morphologies, electrochemical properties and corrosion resistances of the mono and multi-layer coatings were investigated by Fourier-transform infrared spectra, scanning electron microscope, energy dispersive X-ray spectrometer, electrochemical impedance spectroscopy and anodic polarization. Furthermore the geometric structure and electronic properties of indole, aniline, and indole-co-aniline (dimmer) molecules have been investigated by quantum calculations. The results indicated that corrosion protection of copolymers was increased via titanium dioxide pre-coating. The 1:1 copolymer coating showed better corrosion prevention than 1:9 coating. The correlation was determined between experimental and theoretical parameters.

1. Introduction

Recently, new methods have been developed about polymer coating for corrosion protection due to enhancements in the coating performance (Sathiyanarayanan et al., 2007; Lenz et al., 2003; Toprak Doşlü et al., 2013; Baldissera and Ferreira, 2012; Sheng and Ohtsuka, 2012; González et al., 2013; Mathew and Predeep, 2012; Ozyilmaz et al., 2013; Lu et al., 2010). Among these, titanium dioxide (TiO_2) pre-coating is a favourable treatment, because titanium dioxide is one of the most significant transition metal oxides and has excellent chemical stability in both acidic and alkaline solutions. TiO_2 pre-

* Corresponding author. Fax: +90 482 213 40 04.
E-mail address: seraptoprak@artuklu.edu.tr (S.T. Döşlü).
Peer review under responsibility of King Saud University.

Production and hosting by Elsevier

http://dx.doi.org/10.1016/j.arabjc.2017.03.007

coating can operate with several methods but the sol-gel technique has some advantages, such as low processing temperature, homogeneity and low cost (Chen et al., 2007; Seyedjamali and Pirisedigh, 2011a,b; Kierys et al., 2013). Therefore, sol-gel oxide films have a wide range of applications, such as the optically functional materials, microelectronics, and photo-electronics industry, and corrosion protection. In particular, the corrosion performance of organic films has been improved by application of TiO_2 (Qing et al., 2016; Wang et al., 2015; Doğru Mert, 2016; Pagotto et al., 2016).

The corrosion performance can be enhanced not only by TiO_2 sol-gel pre-coating but also by polymer synthesis technique, which is really very important in this field. The electrochemical technique is the most preferred one since it has several advantages, such as enabling the control of different thicknesses of coating, easy preparation of the monomer solutions and the use of the desired monomer concentration. Electrochemical polymerizations of many organic substances, especially including indole, aniline and their derivatives have been studied extensively (Özyılmaz et al., 2005, 2007; Li et al., 1997; Khaled, 2008; Pandey, 1999; Homma et al., 2012; Narayanasamy and Rajendran, 2010; Özyılmaz and Özyilmaz, 2006; Yalcınkaya et al., 2010). These polymers have chemical stability and physical stability at the large range of pH and conductivity. For this reason, these polymers are widely used for corrosion protection and also in many fields such as rechargeable batteries, diodes, transistors, and sensors (Baibarac et al., 2009; Tansuğ et al., 2007).

In this study, TiO_2/poly (indole-co-aniline) multilayer was synthesized with different monomer ratios (1:1 and 1:9) on AISI 304 stainless steel (SS) in 0.15 M lithium perchlorate (LiClO4) containing acetonitrile. The corrosion test was obtained with electrochemical impedance spectroscopy (EIS) and anodic polarization curves in 3.5% NaCl solution. The electrodes were characterized by attenuated total reflectance Fourier-transform infrared spectra (ATR-FTIR), scanning electron microscope (SEM) and energy dispersive X-ray spectrometer (EDX). Furthermore, the geometric structure and electronic properties of molecules have been investigated by DFT method using B3LYP level and 6-311 + +G (d,p) basis set in gas and acetonitrile phases. The quantum calculations were employed and theoretical parameters as energy of the highest occupied molecular orbital (E_{HOMO}), energy of the lowest unoccupied molecular orbital (E_{LUMO}) between LUMO and HOMO and Mulliken charges on the backbone atoms, absolute electronegativity (χ), absolute hardness (η) and the fraction of electrons transferred from the molecule to metal atom (ΔN).

2. Experimental

2.1. Chemicals and apparatus

The indole (In, for synthesis, 99% purity), aniline (An, for synthesis, 99% purity), acetonitrile (ACN, 99.9% purity contains 0.02% water), ethanol (99.9% purity contains 0.1% water) and nitric acid (65% ISO-for analyses) were purchased from Merck Chemicals Company. Titanium butyrate (for synthesis, 97% purity), acrylic acid (99% purity anhydrous) and lithium perchlorate ($LiClO_4$, 99.99% trace metal basis) which have high purity grades were acquired from Fluka Chemicals Company. Electrochemical measurements were carried out by a conventional three-electrode system. The AISI 304 SS electrode was used as working electrode. The chemical composition (wt.%) of SS electrode was 0.057 C, 0.320 Si, 1.900 Mn, 0.038 P, 0.335 S, 17.900 Cr, 8.150 Ni, 0.170 Cu, 0.090 Mo, 71.040 Fe. The SS electrode had a surface area of 0.785 cm^2. The platinum sheet and Ag/AgCl (3 M KCl) electrode were used as a counter electrode (with 2 cm^2 surface area) and reference electrode, respectively. Before each experiment, the SS electrode was mechanically ground with abrasive paper (1200 grade) and cleaned as immersed in a 1:1 acetone: ethanol mixture was risen water. Electrochemical measurements were carried out by a conventional three-electrode system. The electrochemical experiments were performed with CHI 604D electrochemical analyser. The copolymer coatings were synthesized in LiClO4 (0.15 M) + ACN 50 mL solution with monomers. Indole and aniline monomer ratios used (1:1 and 1:9).

2.2. Preparing of TiO_2 pre-coating

The TiO_2 film was coated on the electrode surface by sol-gel technique. The sol-gel method for the preparation of TiO_2 film has been reported in the literature (Toprak Doşlü et al., 2013; Li-qun et al., 2007). TiO_2 sol was prepared by hydrolysis of titanium butyrate ($Ti(OC_4H_9)_{4,}$). One millilitre of titanium butyrate, and 0.8 mL of acrylic acid were stirred with 8.2 mL of ethanol and then the solution was kept for 10 min. After that, the mixture was added to a solution made up 1 mL of nitric acid and 39 mL of distilled water solution at 343 K. Composition of nitric acid solution was calculated 0.361 M. It waited a water bath for 3 h at 343 K. TiO_2 films were prepared by dipping the stainless steel in the sol-gel solution for 5 min. The films on stainless steel were prepared through dipping in the TiO_2 sol–gel solution. This film was kept at room temperature for one day to be dried under atmospheric conditions.

2.3. Electrochemical synthesis of copolymers

All electrochemical syntheses were attained by a cyclic voltammetry technique with the potential range between 0.00 and 1.80 V (vs. Ag/AgCl) and, a scan rate of 50 mV s^{-1}. The copolymer coatings were synthesized in $LiClO_4$ (0.15 M) + ACN 50 mL solution with monomers. Two different monomer ratios of indole and aniline were used for 0.1 M monomer by cyclic voltammetry technique for the synthesis of copolymer steps. After electropolymerization, all coated electrodes were washed distilled water and were dried.

2.4. Characterization of films

The chemical structure of the copolymer was analysed by attenuated total reflectance Fourier-transform infrared (ATR-FTIR) spectrophotometer (Nicolet iS10 FT-IR system). For this purpose, the polymer films were not peeled from the coating surface mechanically. The copolymer films were used directly.

The surface morphologies of copolymer electrodes were studied by scanning electron microscopy (SEM) on LEO 440 microscopes.

The chemical composition of the SS and SS/TiO_2 surface was investigated by energy dispersive X-ray spectrometer (EDX), a part of SEM device.

2.5. Corrosion performance

The corrosion studies of all electrodes were carried out in 3.5% NaCl solution by electrochemical impedance spectroscopy. The corrosion studies were carried out by a conventional three-electrode system. The platinum sheet was used as a

counter electrode. The Ag/AgCl (3 M KCl) electrode was used reference electrode. EIS measurements were recorded at the open-circuit potential (E_{ocp}) in the frequency range from 10^5 to 10^{-3} Hz using the amplitude of 7 mV vs. Ag/AgCl. Z-View2 software was generally used to perform EIS data fitting to an electric equivalent circuit model. Z-View2 fitting software was used for the analysis from the EIS data. The anodic polarization curves were recorded as a function of electrode potential in the anodic direction from the E_{ocp} to 0.8 V vs. Ag/AgCl at a constant sweep rate of 4 mV s^{-1}.

2.6. Theoretical study

It is expected conformity between quantum calculation and experimental studies. Electronic parameters in quantum calculation enable to figure out structure, binding shape, and binding point of molecule. In accordance with this information, explanation can be made about stability of molecule and adherent on surface.

The quantum theoretical calculations were carried out using density functional theory (DFT) with 6-311 + + G (d,p) basis set in gas and ACN phases for all atoms with the Gaussian 09 program. Some electronic properties such as energy of the highest occupied molecular orbital (E_{HOMO}), energy of the lowest unoccupied molecular orbital (E_{LUMO}), energy gap (ΔE) between LUMO and HOMO and Mulliken charges on the backbone atoms, absolute electronegativity (χ), absolute hardness (η) and the fraction of electrons transferred from the molecule to metal atom (ΔN) were determined. The optimized molecular structures and HOMO and LUMO surfaces were visualized using Gauss View.

3. Results and discussion

3.1. Electrochemical synthesis

The electrochemical behaviour of SS and SS/TiO_2 was investigated in $LiClO_4$ + ACN by cyclic voltammetry technique (Fig. 1). There was not any significant electrochemical process occurred on SS electrode in 0.00–1.35 V potential range. After 1.35 V, the current density increased rapidly, possibly due to degradation of the passive film on the stainless steel surface (Tüken et al., 2004). The maximum peak current density was

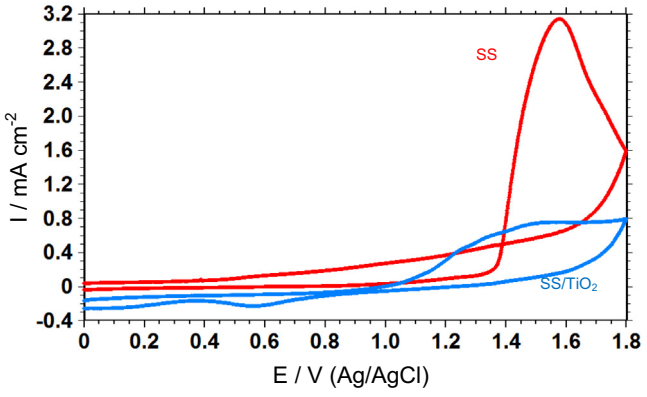

Fig. 1 The cyclic voltammograms of SS and SS/TiO_2 in $LiClO_4$ (0.15 M) + ACN solution; scan rate was 50 mV/s.

3.1 mA cm^{-2}. In Fig. 1, the current density was less than 0.00 mA cm^{-2} until 1.00 V for SS/TiO_2 electrode. After this potential, current density increased probably due to degradation of TiO_2 layer. In Fig. 1, SS/TiO_2 has higher stability than SS in the potential range of 1.00–1.80 V. Sol-gel method made it possible to have a good-quality TiO_2 film coated on SS electrode.

The electrochemical synthesis of copolymer films on SS and SS/TiO_2 is given in Fig. 2. Two different monomer ratios (1:1 and 1:9) were obtained for this purpose. In indole and aniline (1:1) containing solution, the anodic current density increased at 1.40 V in the first cyclic, as expected in the literature (Ozyilmaz et al., 2013; Özyılmaz et al., 2005). Furthermore, the onset of the current density shifted to the lower potential with increasing cycle numbers (Fig. 2). This result can be associated with the formation of a thin copolymer layer that is synthesized in the first cycle with catalysed film growth (Toprak Doşlü et al., 2013). The anodic and cathodic current density peaks showed that the copolymer film could cover the surface successfully (Fig. 2). In indole and aniline (1:9) containing solution, monomer oxidation potential was 1.00 V for the first forward scan. It may illustrate with higher aniline ratio in polymerization solution. It shifted to 1.40 V in the following scans. The anodic current density decreased between 1st and 2nd cycle, and it increased by increasing cycle numbers. The cathodic current increased at 0.90 V in the backward scan. In voltammogram of SS/TiO2/P(In-co-An)(1:9) the shift from nonconducting leucoemeraldine (LE) form to conducting emeraldine (EM) form was determined between 0.20 and 1.20 V in the forward scan (Ozyilmaz et al., 2010). The ia (anodic current density)/ic (cathodic current density) ≈ 1, and the lowest separation between the anodic and cathodic peaks were detected as a result of reversible redox behaviour.

3.2. Characterization of films

The ATR-FTIR spectra showed that the several characteristic peaks were still maintained for each copolymer, which proved that the copolymers were successfully synthesized on stainless steel and TiO_2 coated stainless steel. The FT-IR spectra of two copolymers prepared from solutions containing indole and aniline on SS and SS/TiO_2 were recorded in the range of 1800–650 cm^{-1} in Fig. 3. The band at 1566 cm^{-1} was due to deformation and stretching vibrations of N—H bond (Zhijiang and Guang, 2010; Talbi et al., 1997), which showed that indole did not polymerize through nitrogen. The peaks at 1500 cm^{-1} and 1600 cm^{-1} correspond to —C═C—stretching of reduced and oxidized form of pyrrole rings and benzene rings in indole unit, in all synthesized polymers (Şanlı Aşık et al., 2010). Stretching of —C—N— has been observed between 1450 and 1495 cm^{-1} in the copolymer spectra (Tüken et al., 2004). The peak of pyrrole ring stretching appeared at 1319 cm^{-1} (Doğru Mert et al., 2011). The peak at 1300 cm^{-1} was due to —C—H stretching in plane deformation of pyrrole ring (Doğru Mert et al., 2011). The peak at almost 1100 cm^{-1} was owing to —C═C—H out of plane stretching, which formed during protonation (Baibarac et al., 2009). This peak appeared in copolymers on both surfaces (SS and SS/TiO_2). The peak at nearly 741 cm^{-1} was assigned to benzene ring vibration (Talbi et al., 1997). In addition, peaks of C—H stretching were seen between 850 and

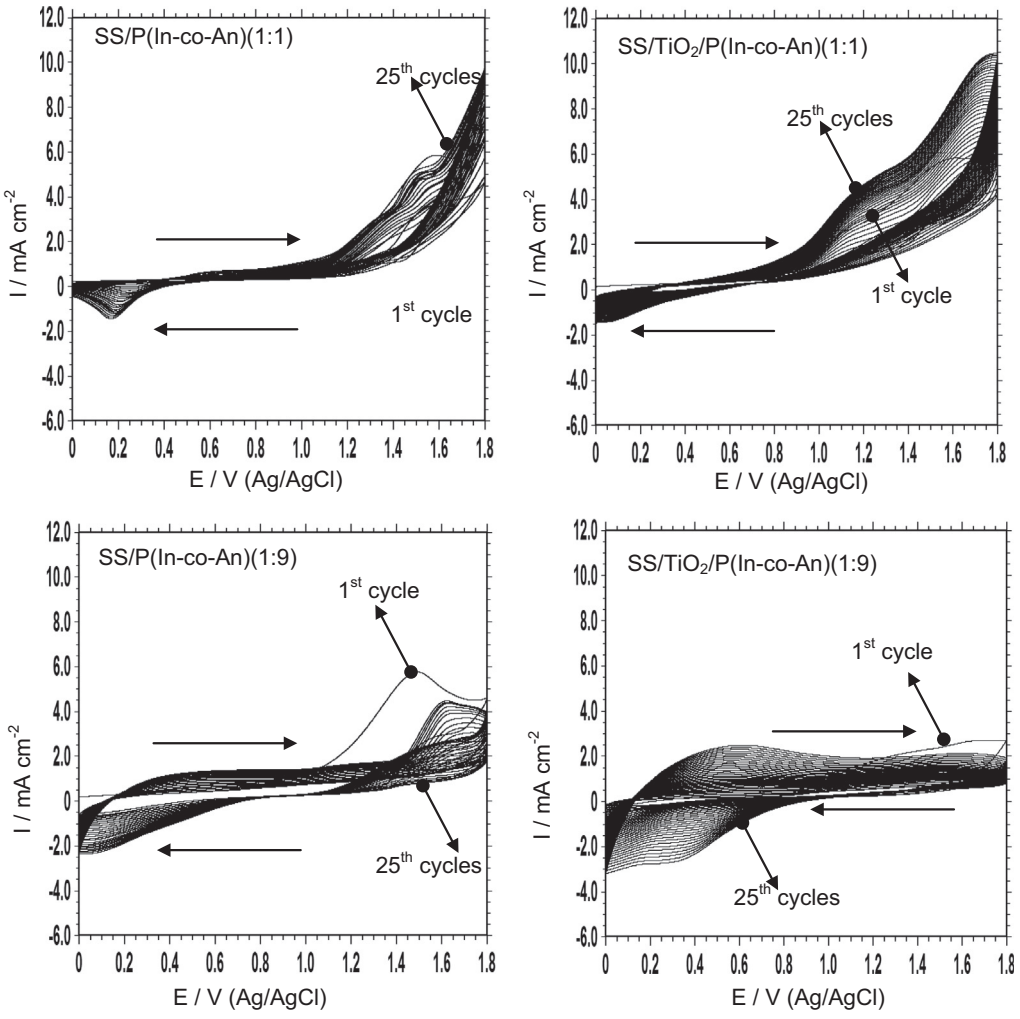

Fig. 2 The synthesis voltammograms of SS/P(In-co-An)(1:1), SS/P(In-co-An)(1:9), SS/TiO_2/P(In-co-An)(1:1) and SS/TiO_2/P(In-co-An)(1:9) in $LiClO_4$ (0.15 M) + ACN solution; scan rate was 50 mV/s.

650 cm^{-1} in the spectra of copolymers (Talbi and Billaud, 1998). The characteristic peaks at about 1625 and 1588 cm^{-1} correspond to the —C═C— stretching vibration in aniline units (Oh and Kim, 2012). The —C═C— bond presents both N═Q═N ring and N—B—N ring. B and Q refer to the benzenoid rings and the quinonoid rings, respectively (Jamadade et al., 2010; Zhou et al., 2007; Tang et al., 2000). These results exhibited that there were still N—H bonds in indole units along the copolymer backbone which implies that copolymerization of indole and aniline occurred between C_3 of indole units and N atom of aniline units (Köleli et al., 2002).

The surface images of all copolymer films are presented in Fig. 4. Copolymers were synthesized on the electrode directly by electrochemical technique. The morphology of copolymer films was deeply affected by two factors as monomer ratio and TiO_2 pre-coating. The morphology of SS/P(In-co-An) (1:1) film showed that the surface was fully covered. The film was frequently stacked, layered and like bark (Fig. 4). The morphology of SS/P(In-co-An)(1:9) copolymer indicated frequently stacked, layered and long strips, while the surface was fully covered (Fig. 4). This implied that, the morphology of the copolymers deals with the monomer ratio. In addition the size of structures in copolymer on TiO_2 coated SS was much smaller than in copolymer on SS. The SS/TiO_2/P(In-co-An)(1:1) named copolymer on the surface of TiO_2 was observed as compact and very regular polymer molecules. The formed films on the surface of TiO_2 were composed of closely-packed and very small molecules. This indicates that the morphology of the synthesized copolymer on SS/TiO_2 was different from SS. As a result of SEM images, the properties of the copolymer have changed by altering monomer ratios. Besides, morphology and adherence of the copolymer showed significant changes with changes on the surface of synthesis.

Fig. 5 presents those EDX measurements of SS (a) and SS/TiO_2 (b) electrode surface. The composition of SS alloy is given in Fig. 5a. There was not any Ti peak detected As seen in Fig. 5a. Fig. 5b exhibited composition of TiO_2 coated SS surface. Ti and O peaks proved that SS surface was coated by TiO_2.

3.3. Corrosion performance

The corrosion behaviour of the uncoated stainless steel (SS), copolymer coated SS electrodes (SS/P(In-co-An)(1:1), SS/P

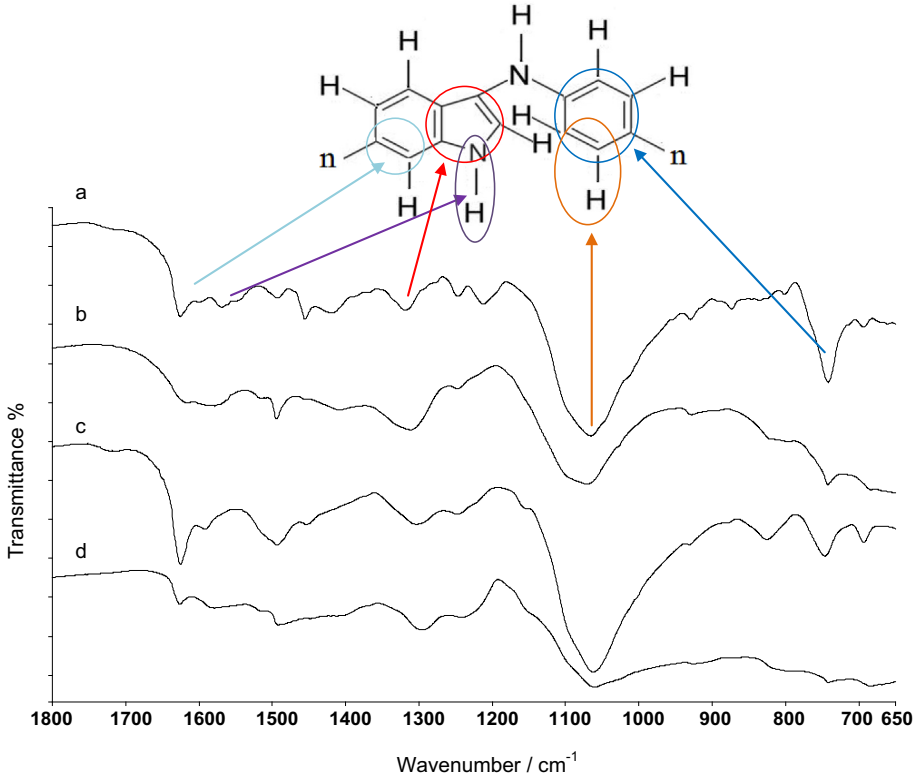

Fig. 3 The FT-IR spectra of SS/P(In-co-An)(1:1) (a), SS/P(In-co-An)(1:9) (b), SS/TiO_2/P(In-co-An)(1:1) (c) and SS/TiO_2/P(In-co-An)(1:9) (d).

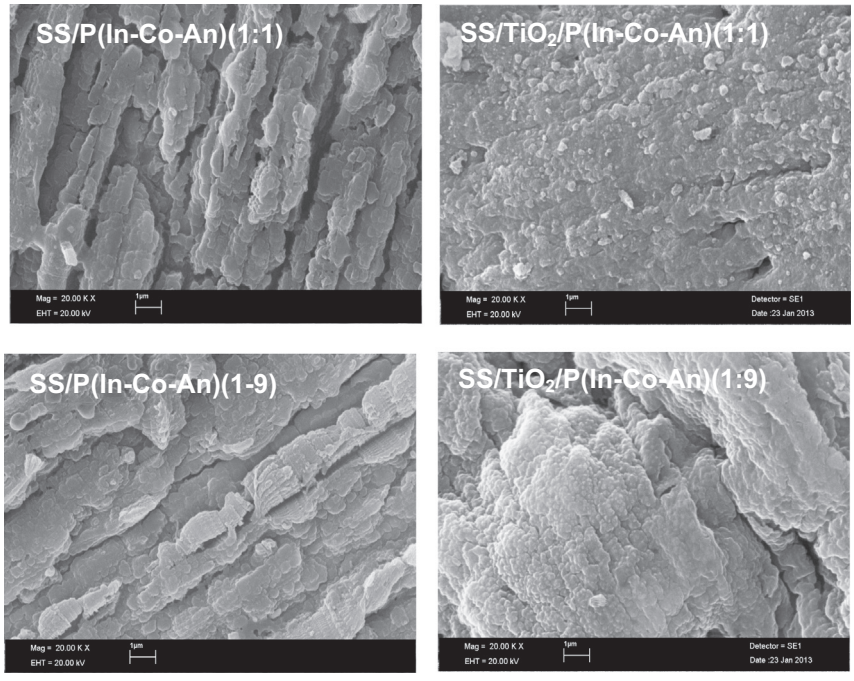

Fig. 4 The SEM micrographs of SS/P(In-co-An)(1:1), SS/P(In-co-An)(1:9), SS/TiO_2/P(In-co-An)(1:1) and SS/TiO_2/P(In-co-An)(1:1).

(In-co-An)(1:9)) and multilayer coatings (SS/TiO_2/P(In-co-An)(1:1), SS/TiO_2/P(In-co-An)(1:9)) was investigated in 3.5% NaCl solution by electrochemical impedance spectroscopy (EIS) after 24 h and 144 h immersion times (Figs. 6 and 7, respectively). The reason for 24 h and 144 h immersion times was that the corrosion behaviour of electrodes in 3.5% NaCl solution was compared between short time (24 h) and long-time (144 h). The equivalent circuit diagram for EIS

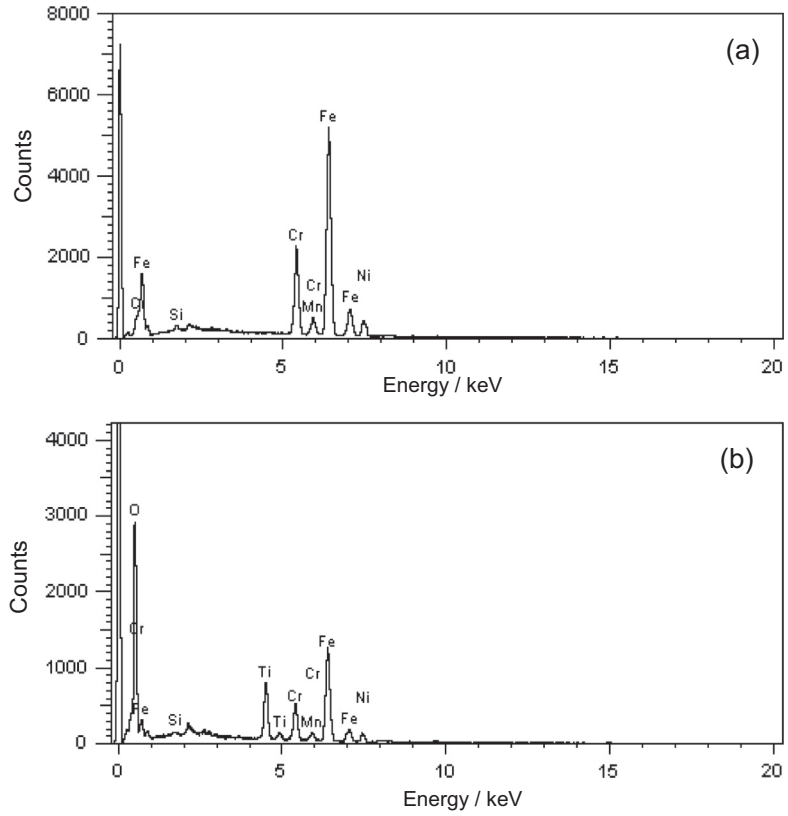

Fig. 5 The EDX spectra of SS (a) and SS/TiO_2 (b) Toprak Doşlü et al., 2013.

measurements is given inset in Fig. 6. In this equivalent circuit R_s, R_p and *CPE* represent the solution resistance, polarization resistance and constant phase element, respectively. The calculated parameters attained from equivalent circuit fitting analysis for all electrodes are given in Table 1.

EIS behaviour of the examined specimens is interpreted based on three distinctive frequency ranges, i.e. a first frequency region is between 10^{-3} Hz and 10^{0} Hz, an intermediate region is between 10^{0} and 10^{4} Hz, and a third region is between 10^{4} and 10^{5} Hz, as also widely reported (Osório et al., 2009, 2011; Rosalbino et al., 2012, 2009). At high-to-medium frequency region a first time constant is commonly observed. At low frequency region (i.e. between 10^{-3} Hz and 10^{0} Hz), a second time constant predominantly occurs (Osório et al., 2009, 2011; Rosalbino et al., 2012, 2009). Into proposed equivalent circuit a CPE is commonly correlated with inhomogeneity, roughness, adsorption of species on surface, and reactivity on surface of the sample (González et al., 2013; Talbi et al., 1997; Ozyilmaz et al., 2010; Zhijiang and Guang, 2010; Köleli et al., 2002). In this context, CPE = [C (j ⟨omega⟩) n] − 1 represents the impedance of a phase element, where C is capacitance; j is the current (imaginary number: −1 0.5); and ⟨omega⟩ is the angular frequency and $-1 \leq n \leq 1$, as widely reported (Osório et al., 2009, 2011; Rosalbino et al., 2012, 2009).

In Fig. 6 single semicircle shaped curves were detected. The R_p value of SS, SS/P(In-co-An)(1:1), SS/P(In-co-An)(1:9), SS/TiO_2/P(In-co-An)(1:1) and SS/TiO_2/P(In-co-An)(1:9) was determined as 16,313, 19,000, 18,000, 24,700, and 23,200 Ω cm^2, respectively. The calculated *CPE* data of SS, SS/P(In-co-An)(1:1), SS/P(In-co-An)(1:9), SS/TiO_2/P(In-co-An)(1:1), and SS/TiO_2/P(In-co-An)(1:9) was 236.5, 163.6, 159.3, 70.2, and 159.1 μF cm^{-2}, respectively. The higher polarization resistance and the lower constant phase element values indicated that copolymer films had barrier effect on SS electrode (Doğru Mert et al., 2011). There exists a number of other references concerning other distinctive system/alloys, which have stated that a decrease in CPE with increase in polarization resistance (charge transfer) induces to the corrosion resistance has been improved (Osório et al., 2009, 2011; Rosalbino et al., 2012, 2009; Liu et al., 2015; Peixoto et al., 2016). However, the SS/TiO_2/P(In-co-An)(1:1) had the higher R_p value and lower *CPE* value than other copolymer coatings. It may be due to strong adherent and less porosity than the other synthesized copolymer film.

After 144 h immersion time, the R_p values for SS, SS/P(In-co-An)(1:1), SS/P(In-co-An)(1:9), SS/TiO_2/P(In-co-An)(1:1), and SS/TiO_2/P(In-co-An)(1:9) were found to be 3500, 15,500, 14,800, 18,800, and 16,500, respectively. As can be seen in Table 1, the polarization resistance decreased when immersion time increased as a result of corrosive effect of chloride ions during immersion. However, another important parameter is *CPE*; it increased with increasing immersion time. The *CPE* of SS, SS/P(In-co-An)(1:1), SS/P(In-co-An)(1:9), SS/TiO_2/P(In-co-An)(1:1), and SS/TiO_2/P(In-co-An)(1:9) was 500.0, 179.1, 227.1, 140.0, and 167.6 μF cm^{-2}, respectively. The decrease in polarization resistance and increase in CPE value during immersion time, showed the decrease in barrier effect of copolymers due to absorbed water in corrosive solutions (Toprak Doşlü et al., 2013; Özyılmaz et al., 2005). Even so, the synthesized copolymer film on TiO_2 coated stainless steel

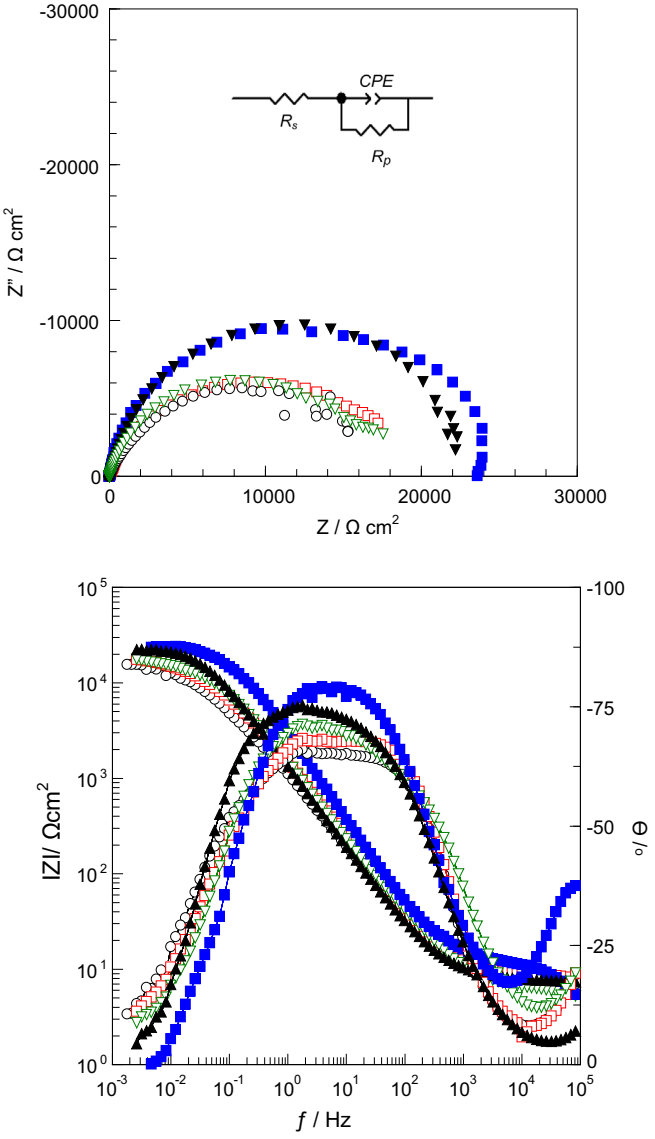

Fig. 6 EIS results of SS(○), SS/P(In-co-An)(1:1)(□), SS/P(In-co-An)(1:9)(▽), SS/TiO_2/P(In-co-An)(1:1)(■), SS/TiO_2/P(In-co-An)(1:9)(▼) after 24 h immersion time. (The equivalent circuit was given inset.)

surface had more resistance against corrosion than the synthesized copolymer film on the bare electrode surface.

Based on the impedance parameters of the examined specimens shown in Table 1, independently of the immersion period considered, the highest Rp is that of the SS/TiO_2/P(In-co-An)(1:1) coating sample. This is followed by the SS/TiO_2/P(In-co-An)(1:1), SS/P(In-co-An)(1:1) and SS/P(In-co-An)(1:9), respectively. The lowest Rp measured is that of the substrate (i.e. SS sample), as expected. Considering an immersion time of 24 h, indistinctively of the considered coating, a corrosion resistance is attained. Besides, indistinctively of 24 h or 144 h, the aforementioned corrosion resistance trend is maintained.

Additionally, the behaviour against corrosion of coatings has also been researched via the anodic polarization measurements. The anodic polarization curves were used to compare stability, efficiencies and physical barrier properties of electrodes under polarized conditions (Yalcınkaya et al., 2008a, b; Doğru Mert and Yazıcı, 2011). These curves are given in Fig. 8. The corrosion potential of SS, SS/P(In-co-An)(1:1), SS/P(In-co-An)(1:9), SS/TiO_2/P(In-co-An)(1:1), and SS/TiO_2/P(In-co-An)(1:9) was 0.08, 0.22, 0.16, 0.29, and 0.27 V, respectively. It was clearly seen that copolymer coated electrodes had noble potential when TiO_2 was used as pre-coating. Furthermore, as seen in Fig. 8 that the copolymer synthesized on SS/TiO_2 had lower current densities than the others and the most protective coating was SS/TiO_2/P(In-co-An)(1:1). The situation revealed was that the physical barrier property of the copolymer on TiO_2 coated surface had increased. In addition, the copolymer on the SS/TiO_2 surface showed better stability at higher potentials. These results were in parallel with EIS measurements.

3.4. Theoretical study

The polymerization mechanism of indole, aniline and their derivatives was studied with the help of spectroscopic and theoretical calculations (Yurtsever and Yurtsever, 2002).

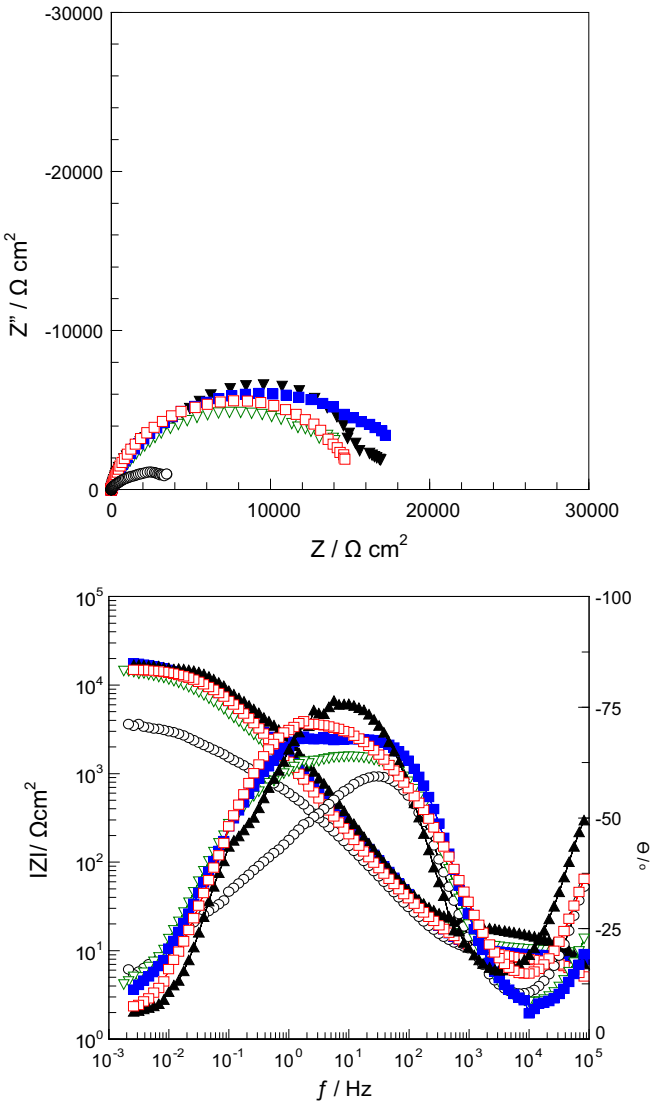

Fig. 7 EIS results of SS(○), SS/P(In-co-An)(1:1)(□), SS/P(In-co-An)(1:9)(▽), SS/TiO_2/P(In-co-An)(1:1)(■), SS/TiO_2/P(In-co-An)(1:9)(▼) after 144 h immersion time.

Researchers (Yurtsever and Yurtsever, 2002; Köleli and Dündar, 2008) declared that indole is polymerized on 1–3 positions, 3–6 positions, 2–3 positions and 3–3, 2–2 couplings. The aniline is polymerized with N bridge; most forms of polyaniline are one of the three states or physical mixtures of these components. Leucoemeraldine (LE) is the fully reduced state. Pernigraniline (PE) is the fully oxidized state with imine links instead of amine links. The emeraldine form of polyaniline, often referred to as emeraldine base (EB), is neutral, and if doped it is called emeraldine salt (ES), with the imine nitrogen protonated by an acid. Protonation helps to delocalize the otherwise trapped diiminoquinone-diaminobenzene state.

In this study, theoretical calculations were operated due to given detailed information about polymerization mechanism. The calculations of indole, aniline, and indole-co-aniline were performed for the gas phase of molecule and the acetonitrile phases. The Mulliken charges on the backbone atoms, the highest occupied molecular orbital (E_{HOMO}), energy of the lowest unoccupied molecular orbital (E_{LUMO}), energy gap (ΔE) between LUMO and HOMO, dipole moment, etc., were determined and are given in Table 2. According to the Mulliken charges of indole and aniline, polymerization may occur over positions 3–6 of indole molecule and over the nitrogen and para-position of aniline (Fig. 9). Köleli and Dündar (Köleli and Dündar, 2008) suggested that polymerization of indole-aniline occurs over the nitrogen atom and the para-position of the aniline ring. They discussed three possibilities to obtain the structure of the copolymer. In all cases, whichever mechanism is considered, it leads to the same product and further electron transfer steps lead to the polymerization of these species. The reacting predisposition of molecules is associated with their frontier molecular orbitals, the HOMO and LUMO. Higher HOMO energy (E_{HOMO}) of the molecule means a higher electron donating ability to appropriate acceptor molecules with low energy empty molecular orbital (Arslan et al., 2009; Ghailane et al., 2013). The calculated E_{HOMO} in

Table 1 Electrochemical parameters for electrodes corresponding to the EIS data obtained in 3.5% NaCl solution after 24 h and 144 h immersion times.

Electrode	*t*/h	$R_p/\Omega\ cm^2$	$CPE/\mu F\ cm^{-2}$	*n*	*chi-squared*
SS	24	16,313	236.5	0.75	1.4×10^{-3}
	144	3500	500.0	0.72	2.0×10^{-3}
SS/TiO_2	24	31,889	150.6	0.85	1.8×10^{-3}
	144	19,972	151.3	0.82	1.6×10^{-3}
SS/P(In-co-An)(1:1)	24	19,000	163.6	0.73	2.9×10^{-3}
	144	15,500	179.1	0.80	4.9×10^{-3}
SS/TiO_2/P(In-co-An)(1:1)	24	24,700	70.2	0.86	7.2×10^{-3}
	144	18,800	140.0	0.77	2.8×10^{-3}
SS/P(In-co-An)(1:9)	24	18,000	159.3	0.80	2.7×10^{-3}
	144	14,800	227.1	0.76	3.2×10^{-3}
SS/TiO_2/P(In-co-An)(1:9)	24	23,200	159.1	0.88	1.7×10^{-3}
	144	16,500	167.6	0.88	9.2×10^{-3}

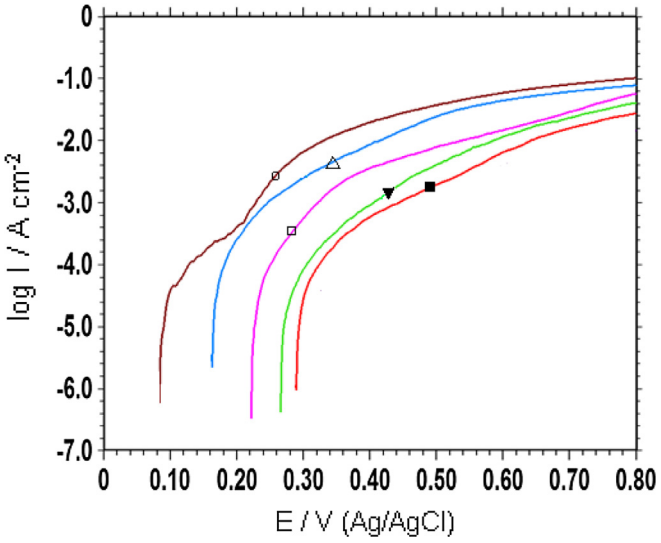

Fig. 8 Polarization plots of SS(——), SS/P(In-co-An)(1:1)(——), SS/P(In-co-An)(1:9)(——), SS/TiO_2/P(In-co-An)(1:1)(——), SS/TiO_2/P(In-co-An)(1:9)(——) after 144 h immersion time.

Table 2 The calculated quantum parameters for monomers and dimer molecules in gas and ACN phases.

	Indole		Aniline		In-co-ani	
	Gas	ACN	Gas	ACN	Gas	ACN
E_{HOMO}/eV	−5.801	−5.935	−5.781	−5.909	−5.085	−5.167
E_{LUMO}/eV	−0.619	−0.776	−0.365	−0.522	−0.809	−0.882
μ/Debye	2.132	2.973	1.592	2.076	1.974	2.764
χ/eV	3.210	3.356	3.073	3.216	2.947	3.025
η/eV	2.591	2.800	2.708	2.694	2.138	2.143
Δ*N*	0.731	0.651	0.725	0.702	0.948	0.927

gas phase were −5.801, −5.781 and −5.085 eV, for indole, aniline and indole-co-aniline respectively. The values were significantly changed in ACN phase, −5.935, −5.909 and −5.167 eV, respectively. The LUMO energy (E_{LUMO}) indicates the electron accepting ability of the molecules, the lowest its value the higher the capability of accepting electrons. The gap energy between the frontier orbitals (Δ*E*) is the important factor in describing the molecular activity, so when the gap

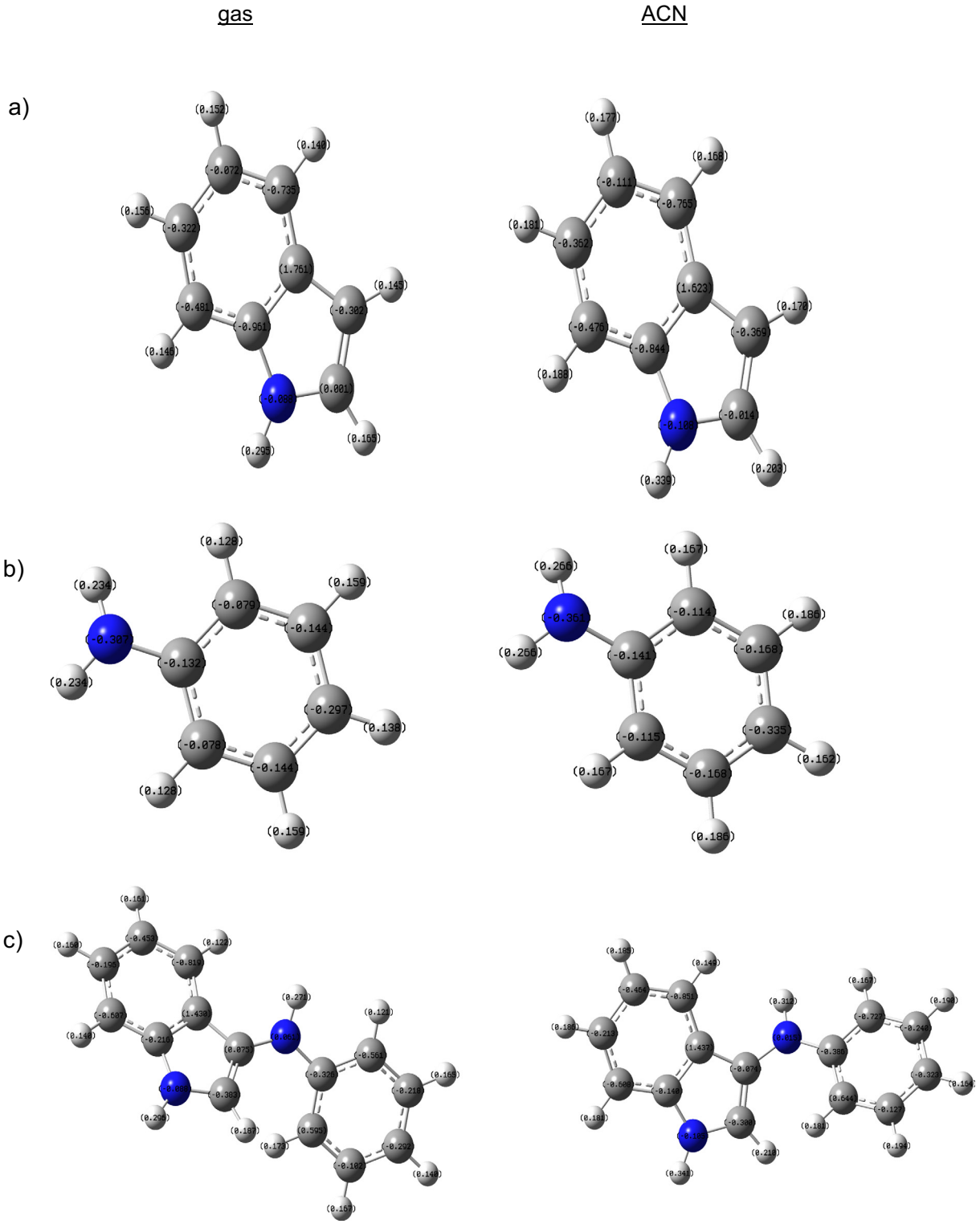

Fig. 9 Mulliken charge values of indole (a), aniline (b) and indole-co-aniline (c) in gas and ACN phases.

energy decreased, the adsorption ability is improved (Ghailane et al., 2013) because the energy to remove an electron from the last occupied orbital will be low (Gece and Bilgiç, 2009). The minimum E_{LUMO} and ΔE were determined for indole-co-aniline in Table 2. The high dipole moment of molecules in ACN phase, probably indicates strong dipole–dipole interactions between solvated molecule and metallic surface, so more adherent coatings may occur. According to the literature, absolute electronegativity (χ), absolute hardness (η) and the fraction of electrons transferred from the molecule to metal

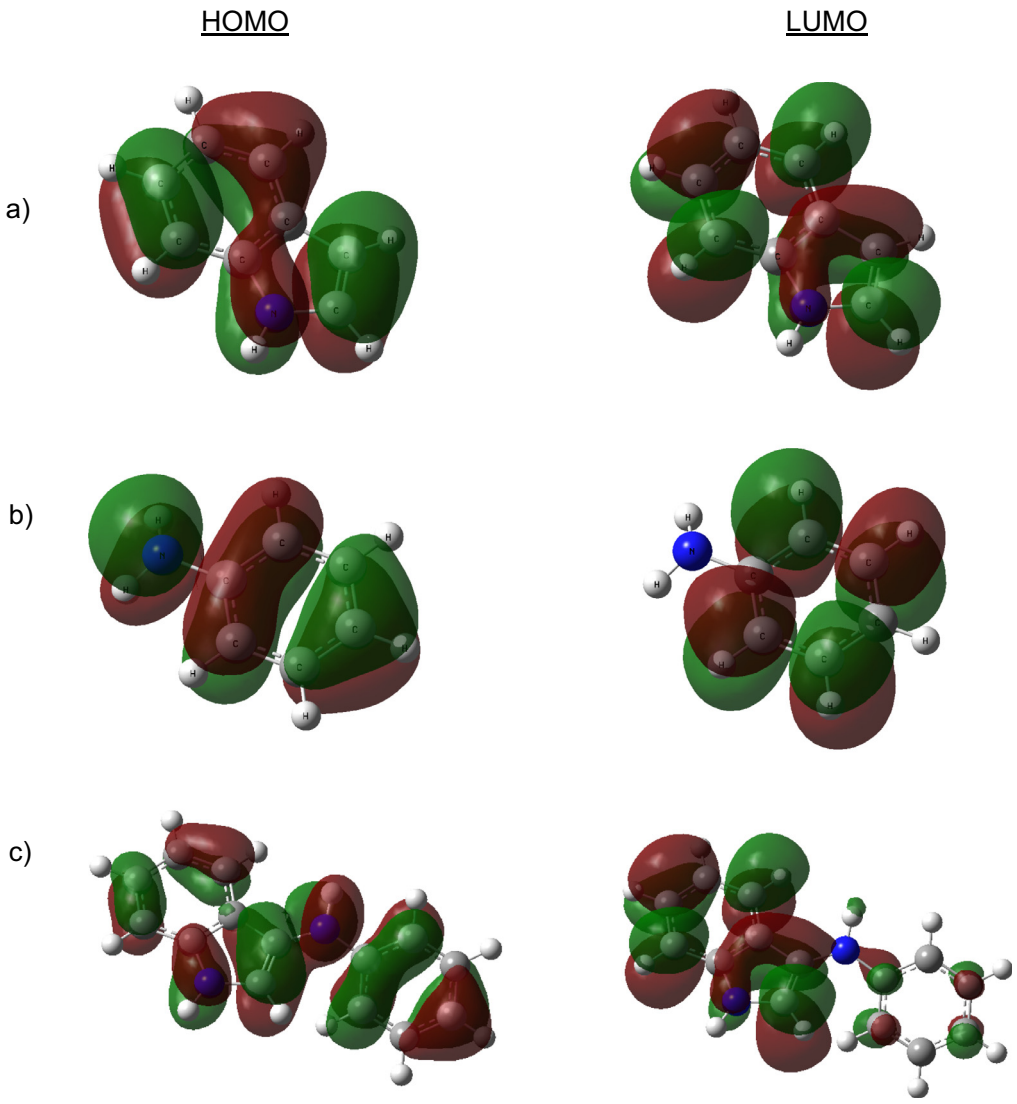

Fig. 10 HOMO and LUMO orbitals of indole (a), aniline (b) and indole-co-aniline (c) in gas and ACN phases.

atom (ΔN) imply the interaction between metal and molecules. The highest χ and η values were determined for indole and the highest ΔN value was determined for indole-co-aniline Fig. 10.

4. Conclusion

The copolymer films based on indole and aniline with two different monomer feed ratios were synthesized on stainless steel (SS) and TiO_2 coated stainless steel. It was found that TiO_2 coating was necessary for a good-quality copolymer film synthesis. The synthesized copolymers on SS/TiO_2 exhibited better barrier effect because TiO_2 coating exhibited significant physical barrier behaviour on SS. In addition, the indole-aniline copolymer that was prepared at 1:1 ratio was determined more stable against corrosion. As a result, the best barrier effect was detected for TiO_2 pre-coated copolymer (P(In-co-An)(1:1)) due to high resistance and low CPE values, even after 144 h immersion time. Experimental and theoretical experiments indicate that, polymerization of indole-aniline occurs over the nitrogen atom and the para-position of the aniline ring. The χ, η and ΔN values were signalled and the polymer stability may be improved with increasing indole monomer ratio.

This study showed that, this new multilayer coating will find wide application areas due to high corrosion resistance and characteristic chemical and physical properties.

Acknowledgments

This study has been financially supported by the Çukurova University research fund. The authors are greatly thankful to Çukurova University Research fund (Project Number: FEF2010D20).

References

Arslan, T., Kandemirli, F., Ebenso, E.E., Love, I., Alemu, H., 2009. Quantum chemical studies on the corrosion inhibition of some sulphonamides on mild steel in acidic medium. Corros. Sci. 51, 35–47.

Baibarac, M., Baltog, I., Scocioreanu, M., Lefrant, S., Mevellec, J.Y., 2009. Vibrational properties of the electrochemically synthesized polyindole/single-walled carbon nanotubes composite. Synth. Met. 159, 2550–2555.

Baldissera, A.F., Ferreira, C.A., 2012. Coatings based on electronic conducting polymers for corrosion protection of metals. Prog. Org. Coat. 75, 241–247.

Chen, L., Shen, H., Lu, Z., Feng, C., Chen, S., Wang, Y., 2007. Fabrication and characterization of TiO_2–SiO_2 composite nanoparticles and polyurethane/(TiO_2–SiO_2) nanocomposite films. Colloid Polym. Sci. 285, 1515–1520.

Doğru Mert, B., 2016. Corrosion protection of aluminum by electrochemically synthesized composite organic coating. Corros. Sci. 103, 88–94.

Doğru Mert, B., Yazıcı, B., 2011. The electrochemical synthesis of poly (pyrrole-co-o-anisidine) on 3102 aluminum alloy and its corrosion protection properties. Mater. Chem. Phys. 125, 370–376.

Doğru Mert, B., Solmaz, R., Kardaş, G., Yazıcı, B., 2011. Copper/polypyrrole multilayer coating for 7075 aluminum alloy protection. Prog. Org. Coat. 72, 748–754.

Gece, G., Bilgiç, S., 2009. Quantum chemical study of some cyclic nitrogen compounds as corrosion inhibitors of steel in NaCl media. Corros. Sci. 51, 1876–1878.

Ghailane, T., Balkhmima, R.A., Ghailane, R., Souizi, A., Touir, R., Ebn Touhami, M., Marakchi, K., Komiha, N., 2013. Experimental and theoretical studies for mild steel corrosion inhibition in 1 M HCl by two new benzothiazine derivatives. Corros. Sci. 76, 317–324.

González, M.B., Brugnoni, L.I., Vela, M.E., Saidman, S.B., 2013. Silver deposition on polypyrrole films electrosynthesized in salicylate solutions. Electrochim. Acta 102, 66–71.

Homma, T., Kondo, M., Kuwahara, T., Shimomura, M., 2012. Electrochemical polymerization of aniline in the presence of poly (acrylic acid) and characterization of the resulting films. Polymer 53, 223–228.

Jamadade, V.S., Dhawale, D.S., Lokhande, C.D., 2010. Studies on electrosynthesized leucoemeraldine, emeraldine and pernigraniline forms of polyaniline films and their supercapacitive behavior. Synth. Met. 160, 955–960.

Khaled, K.F., 2008. Application of electrochemical frequency modulation for monitoring corrosion and corrosion inhibition of iron by some indole derivatives in molar hydrochloric acid. Mater. Chem. Phys. 112, 290–300.

Kierys, A., Zaleski, R., Buda, W., Pikus, S., Dziadosz, M., Goworek, J., 2013. Nanostructured polymer–titanium composites and titanium oxide through polymer swelling in titania precursor. Colloid Polym. Sci. 291, 1463–1470.

Köleli, F., Dündar, D., 2008. Synthesis, characterization and SEESR spectroscopic investigations of indole/aniline copolymers. J. Appl. Polym. Sci. 109, 3044–3049.

Köleli, F., Arslan, Y., Düdükcü, M., 2002. Preparation and SEESR-spectroscopic investigations of indole/pyrrole copolymers in aprotic medium. Synth. Met. 129, 47–52.

Lenz, D.M., Delamar, M., Ferreira, C.A., 2003. Application of polypyrrole/TiO_2 composite films as corrosion protection of mild steel. J. Electroanal. Chem. 540, 35–44.

Li, P., Tan, T.C., Lee, J.Y., 1997. Corrosion protection of mild steel by electroactive polyaniline coatings. Synth. Met. 88, 237–242.

Li-qun, M., Qing-lin, L., Zhi-jun, Z., 2007. Study on surface states of Pt/TiO_2 thin film in different atmospheres. Solar Energy 81, 1280–1284.

Liu, J.C., Zhang, G., Ma, J.S., Suganuma, K., 2015. Ti addition to enhance corrosion resistance of Sn-Zn solder alloy by tailoring microstructure. J. Alloys Compounds 644, 113–118.

Lu, G., Li, Y., Lu, C., Xu, Z., 2010. Corrosion protection of iron surface modified by poly(methyl methacrylate) using surface-initiated atom transfer radical polymerization (SI-ATRP). Colloid Polym. Sci. 288, 1445–1455.

Mathew, A.M., Predeep, P., 2012. Styrene butadiene co-polymer based conducting polymer composite as an effective corrosion protective coating. Prog. Org. Coat. 74, 14–18.

Narayanasamy, B., Rajendran, S., 2010. Electropolymerized bilayer coatings of polyaniline and poly(N-methylaniline) on mild steel and their corrosion protection performance. Prog. Org. Coat. 67, 246–254.

Oh, M., Kim, S., 2012. Synthesis and electrochemical analysis of polyaniline/TiO_2 composites prepared with various molar ratios between aniline monomer and para-toluenesulfonic acid. Electrochim. Acta 78, 279–285.

Osório, W.R., Cheung, N., Peixoto, L.C., Garcia, A., 2009. Corrosion resistance and mechanical properties of an al 9wt%Si alloy treated by laser surface remelting. Int. J. Electrochem. Sci. 4, 820–831.

Osório, W.R., Garcia, L.R., Peixoto, L.C., Garcia, A., 2011. Electrochemical behavior of a lead-free SnAg solder alloy affected by the microstructure array. Mater. Des. 32, 4763–4772.

Özyılmaz, A.T., Özyilmaz, G., 2006. Novel synthesis medium for poly (aniline-co-*o*-anisidine). Surf. Coat. Technol. 201, 2484–2490.

Özyılmaz, A.T., Colak, N., Sangün, M.K., Erbil, M., Yazıcı, B., 2005. The electrochemical synthesis of poly(aniline-*co*-*o*-anisidine) on copper and their corrosion performances. Prog. Org. Coat. 54, 353–359.

Özyılmaz, A.T., Çolak, N., Özyilmaz, G., Sangün, M.K., 2007. Protective properties of polyaniline and poly(aniline-co-*o*-anisidine) films electrosynthesized on brass. Prog. Org. Coat. 60, 24–32.

Ozyilmaz, A.T., Ozyilmaz, G., Yigitoglu, O., 2010. Synthesis and characterization of poly(aniline) and poly(o-anisidine) films in sulphamic acid solution and their anticorrosion properties. Prog. Org. Coat. 67, 28–37.

Ozyilmaz, A.T., Akdag, A., Karahan, I.H., Ozyilmaz, G., 2013. The influence of polyaniline (PANI) coating on corrosion behaviour of zinc–cobalt coated carbon steel electrode. Prog. Org. Coat. 76, 993–997.

Pagotto, J.F., Recio, F.J., Motheo, A.J., Herrasti, P., 2016. Multilayers of PAni/n-TiO_2 and PAni on carbon steel and welded carbon steel for corrosion protection. Surf. Coat. Technol. 289, 23–28.

Pandey, P.C., 1999. Copper (II) ion sensor based on electropolymerized undoped-polyindole modified electrode. Sens. Actuators, B: Chem. 54, 210–214.

Peixoto, L.C., Bortolozo, A.D., Garcia, A., Osório, W.R., 2016. Performance of new Pb-Bi alloys for Pb-Acid battery applications: EIS and polarization study. J. Mater. Eng. Perform. 25, 2211–2221.

Qing, Y., Yang, C., Yu, N., Shang, Y., Sun, Y., Wang, L., Liu, C., 2016. Superhydrophobic TiO_2/polyvinylidene fluoride composite surface with reversible wettability switching and corrosion resistance. Chem. Eng. J. 290, 37–44.

Rosalbino, F., Angelini, E., Zanicchi, G., Carlini, R., Marazza, R., 2009. Electrochemical corrosion study of Sn-3Ag-3Cu solder alloy in NaCl solution. Electrochim. Acta 54, 7231–7235.

Rosalbino, F., Zanicchi, G., Carlini, R., Angelini, E., Marazza, R., 2012. Electrochemical corrosion behaviour of Sn-Ag-Cu (SAC) eutectic alloy in a chloride containing environment. Mater. Corros. 63, 492–496.

Şanlı Aşık, N., Taş, R., Sönmezoğlu, S., Can, M., Çankaya, G., 2010. Monomer effect on stability, electrical conductivity and combination of aniline–indole copolymer synthesized with H_5IO_6 Monomer effect on stability, electrical conductivity and combination of aniline–indole copolymer synthesized with H_5IO_6. J. Non-Cryst. Solids 356, 1848–1853.

Sathiyanarayanan, S., Syed Azim, S., Venkatachari, G., 2007. Corrosion protection of magnesium ZM 21 alloy with polyaniline–TiO_2 composite containing coatings. Prog. Org. Coat. 59, 291–296.

Seyedjamali, H., Pirisedigh, A., 2011. In situ sol–gel fabrication of new poly(amide–ether–imide)/titania (TiO_2) nanocomposite thin films containing L-leucine moieties. Colloid Polym. Sci. 289, 15–20.

Seyedjamali, H., Pirisedigh, A., 2011. Well-dispersed polyimide/TiO_2 nanocomposites: in situ sol–gel fabrication and morphological study. Colloid Polym. Sci. 290, 653–659.

Sheng, N., Ohtsuka, T., 2012. Preparation of conducting poly-pyrrole layer on zinc coated Mg alloy of AZ91D for corrosion protection. Prog. Org. Coat. 75, 59–64.

Talbi, H., Billaud, D., 1998. Electrochemical properties of polyindole and poly(5-cyanoindole) in $LiClO_4$—acetonitrile and in HCl and $HClO_4$ solutions. Synth. Met. 93, 105–110.

Talbi, H., Humbert, B., Billaud, D., 1997. Polyindole and poly(5-cyanoindole): electrochemical and FT-IR spectroscopic comparative studies. Synth. Met. 84, 875–876.

Tang, Z., Liu, S., Wang, Z., Dong, S., Wang, E., 2000. Electrochemical synthesis of polyaniline nanoparticles. Electrochem. Commun. 2, 32–35.

Tansuğ, G., Tüken, T., Özyılmaz, A.T., Erbil, M., Yazıcı, B., 2007. Mild steel protection with epoxy top coated polypyrrole and polyaniline in 3.5% NaCl. Curr. Appl. Phys. 7, 440–445.

Toprak Doşlü, S., Doğru Mert, B., Yazıcı, B., 2013. Polyindole top coat on TiO_2 sol-gel films for corrosion protection of steel. Corros. Sci. 66, 51–58.

Tüken, T., Özyılmaz, A.T., Yazıcı, B., Erbil, M., 2004. Electrochemical synthesis of polyaniline on mild steel in acetonitrile–$LiClO_4$ and corrosion performance. Appl. Surf. Sci. 236, 292–305.

Tüken, T., Yazıcı, B., Erbil, M., 2004. The use of polythiophene for mild steel protection. Prog. Org. Coat. 51, 205–212.

Wang, N., Fu, W., Zhang, J., Li, X., Fang, Q., 2015. Corrosion performance of waterborne epoxy coatings containing polyethylenimine treated mesoporous-TiO_2 nanoparticles on mild steel. Prog. Org. Coat. 89, 114–122.

Yalcınkaya, S., Tuken, T., Yazıcı, B., Erbil, M., 2008a. Electrochemical synthesis and corrosion performance of poly(pyrrole-co-*o*-anisidine). Prog. Org. Coat. 62, 226–244.

Yalcınkaya, S., Tuken, T., Yazıcı, B., Erbil, M., 2008b. Electrochemical synthesis and characterization of poly(pyrrole-*co*-*o*-toluidine). Prog. Org. Coat. 63, 424–433.

Yalcınkaya, S., Tuken, T., Yazıcı, B., Erbil, M., 2010. Electrochemical synthesis and corrosion behaviour of poly (pyrrole-*co*-*o*-anisidine-*co*-*o*-toluidine). Curr. Appl. Phys. 10, 783–789.

Yurtsever, M., Yurtsever, E., 2002. A DFT study of polymerization mechanisms of indole. Polymer 43, 6019–6025.

Zhijiang, C., Guang, Y., 2010. Synthesis of polyindole and its evaluation for Li-ion battery applications. Synth. Met. 160, 1902–1905.

Zhou, S., Wu, T., Kan, J., 2007. Effect of methanol on morphology of polyaniline. Eur. Polym. J. 43, 395–402.